RAA 2018 Vol. **18** No. **12**, 158(6pp) doi: 10.1088/1674–4527/18/12/158

http://www.raa-journal.org *http://iopscience.iop.org/raa*

***R**esearch in*
***A**stronomy and*
***A**strophysics*

The simplest way to get a cluster's parameters in the *Gaia* era (Dolidze 41)

Ashraf Latif Tadross

National Research Institute of Astronomy & Geophysics, 11421-Helwan, Cairo, Egypt; *altadross@yahoo.com*

Received 2018 July 11; accepted 2018 August 5

Abstract The astro-photometric parameters of the open star cluster Dolidze 41, which is located in the constellation Cygnus, have been investigated using the *Gaia* DR2 large survey that is merged with the near infrared Two Micron All Sky Survey (2MASS) database. The radial density distribution (limited, core and tidal radii), color-magnitude diagrams, galactocentric coordinates, distances, color excess and age of Dolidze 41 are presented. The *Gaia* DR2 astrometry helped us to define the membership of the cluster stars easily. The luminosity and mass functions, the entire luminosity and mass, and the relaxation time of the cluster have been estimated as well.

Key words: (Galaxy:) open clusters and associations: individual (Dolidze 41) — photometry: Color-Magnitude Diagram — astrometry — stars: luminosity function, mass function — astronomical data bases: miscellaneous

1 INTRODUCTION

One of the foremost necessary constituents in studying the structure and evolution of the Milky Way system is star clusters. Known stellar clusters comprise about 160 globular clusters and about 3000 open clusters (Kharchenko et al. 2013). If we extrapolate the solar vicinity to the whole disc, we may reach about 100 000 open clusters (Bragaglia 2018). Many such objects are newly discovered and need photometric investigations, as well as confirmation regarding their physical nature. We believe that most of them will be detected and investigated in the *Gaia* Data Release 2 (DR2) era. The name *Gaia* was originally derived as an acronym for *Global Astrometric Interferometer for Astrophysics*. This referred to the optical technique of interferometry that was originally planned for use on the spacecraft. Although the working method evolved during studies and the acronym is no longer applicable, the name *Gaia* remained to provide continuity with the project. It is the backbone in the science program administered by the European Space Agency (ESA), which launched *Gaia* on 2013 December 19. *Gaia* is situated 1.5 million km from Earth. The spacecraft has monitored each of its target objects about 70 times to a magnitude of G = 20 over a period of five years to study the precise position and motion of each one. *Gaia* DR2 was released on 2018 April 25 for 1.7 billion sources, which provides exquisite precision with astrometric five-parameter solutions of coordinates, proper motions in right ascension and declination, and parallaxes (α, δ, $\mu_\alpha \cos\delta$, μ_δ, π). In addition, magnitudes have been acquired in three photometric filters ($G, G_{\rm BP}, G_{\rm RP}$) for more than 1.3 billion sources (Gaia Collaboration et al. 2018). The *Gaia* Archive is available through the web page *http://www.cosmos.esa.int/gaia*.

With the help of the Virtual Observatory tools TOPCAT and ALADIN we could use the cross-matched data of *Gaia* DR2 and the 2MASS survey to compile useful photometrical data to investigate Dolidze 41 (Bonnarel et al. 2000; Taylor 2005). The current work is part of our continuing series whose goal is to get the most astrophysical properties of newly, antecedently unstudied and/or poorly studied open clusters utilizing the foremost new databases (Tadross 2008b,a, 2009a,b, 2011). The most important aspect of using *Gaia* DR2 with the survey lies in the positions, parallax and proper motions for the cluster stars, which makes the member candidates easily determinable.

J2000.0 coordinates of Dolidze 41 are $\alpha = 20^{\rm h}18^{\rm m}49^{\rm s}$, $\delta = +37°45'00''$, $\ell = 75.707°$ and $b = 0.9925°$ in the constellation Cygnus with a rough angular size of $12'$ as shown in Figure 1. Kazlauskas et al.

Fig. 1 The image of Dolidze 41 as taken from ALADIN. $\alpha = 20^{\rm h}\ 18^{\rm m}\ 49^{\rm s}$, $\delta = +37^\circ 45' 00''$, $\ell = 75.707^\circ$ and $b = 0.9925^\circ$. North is up and East is to the left.

(2013) and Dias et al. (2014) mentioned some updated astrometric information about the cluster. No real photometric data have been published for Dolidze 41 to date except the study of Tadross & Nasser (2010), hereafter TN (2010). In the present work, we re-study Dolidze 41 applying *Gaia* DR2. Near-infrared *JHK* photometry from the 2MASS catalog of Skrutskie et al. (2006) is also used to estimate and confirm most of the main properties of the cluster.

This paper is arranged as follows. The target data are presented in Section 2. The radial density profile is described in Section 3. Color-magnitude diagrams (CMDs) are presented in Section 4. Luminosity and mass functions, and the dynamical status of the cluster, are discussed in Section 5. Finally, the conclusion of the present study is given in Section 6.

2 TARGET DATA

Using TOPCAT, 12 625 sources were downloaded from the *Gaia* DR2 database service within an area of $10'$ located at the center of the cluster, while 6097 near-infrared sources were downloaded from the 2MASS database service (Skrutskie et al. 2006) for the same area of the cluster. Both data were cross-matched, yielding 5570 sources which contain all the data we need. Among the *Gaia* DR2-2MASS cross-matched sources, a subset of 480 stars around the cluster center were selected as comoving stars (the stars that travel together in the same direction through space) with a halo-like background field (Bragaglia 2018), as shown in Figure 2. For those comoving stars, the mean values and standard deviations of $\mu_\alpha \cos\delta$ and μ_δ were found to be –2.95 $\pm$ 0.14 mas yr^{-1} and –4.68 $\pm$ 0.14 mas yr^{-1} respectively, as shown in Figure 3. Stars are considered cluster member candidates if their 3σ parallax error lies within the cluster mean parallax of 0.23 $\pm$ 0.06 mas, and are located in the range of 0.1 mas $< \pi <$ 0.4 mas. Stars were selected to be cluster member candidates which have almost the same speed and direction in the sky with respect to the fore/background field ones, and at the same time are located within the limited size of the cluster, see Figure 4.

3 RADIAL DENSITY PROFILE

Radius determination is one of the most important fundamental properties of the cluster. To determine the cluster's limited radius and core radius, the radial surface density of the stars $\rho(r)$ should be firstly calculated. In this context, stars inside the area of Dolidze 41 are counted in concentric rings outwards from the cluster center with equal increments in radius of $0.1'$.

Figure 5 shows the radial density profile of the cluster, where the mean stellar density in each ring is plotted against the corresponding average radius. The cluster's limited border is taken at the point which comprises the entire cluster area and achieves sufficient stability with the background field density, i.e. at the point where cluster stars dissolve into the background field; for more details see Tadross (2011). Applying the empirical King's Model (King 1966), the density function $\rho(r)$ is represented as

$$\rho(r) = f_{\rm bg} + \frac{f_0}{1 + (r/r_{\rm c})^2} \ , \tag{1}$$

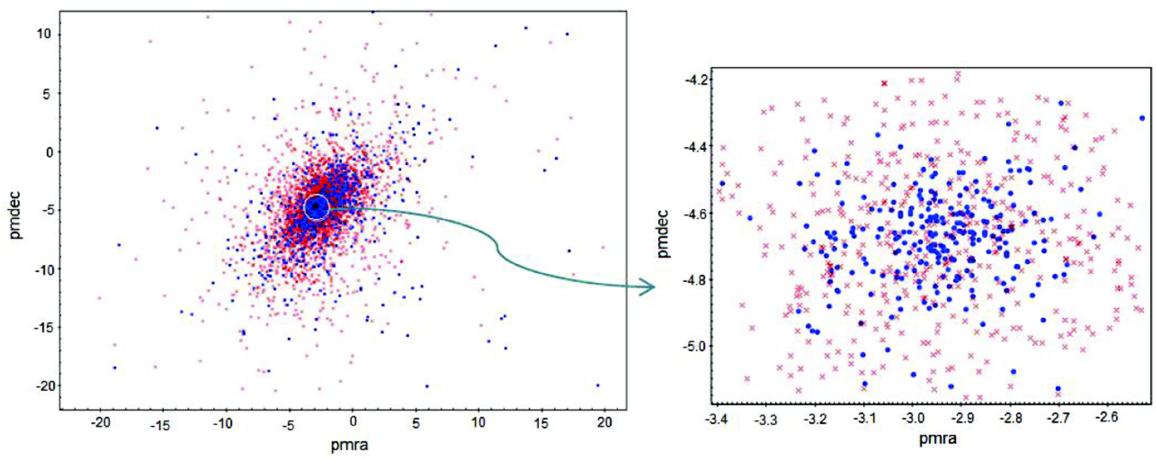

Fig. 2 The left panel displays the proper motion diagram for Dolidze 41. The *red crosses* refer to the concentrated field with a halo-like background field, while the *blue dots* show stars with proper motion errors less than 10%. The *white circle* indicates the studied cluster's area, in which 480 co-moving stars are located as shown in the enlarged view of the right panel.

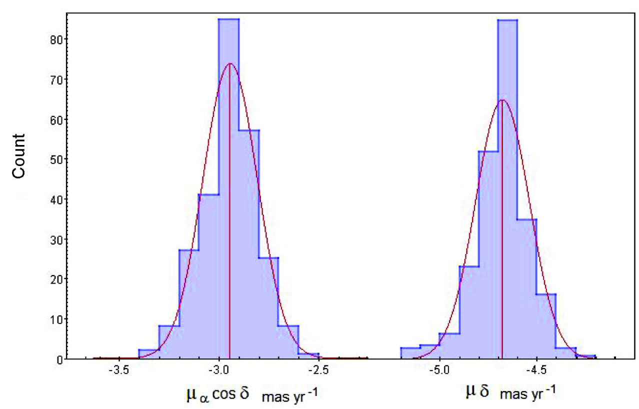

Fig. 3 The mean values and standard deviations of $\mu_\alpha \cos\delta$ and μ_δ for the cluster member candidates, which are found to be –2.95 $\pm$ 0.14 mas yr^{-1} and –4.68 $\pm$ 0.14 mas yr^{-1} respectively.

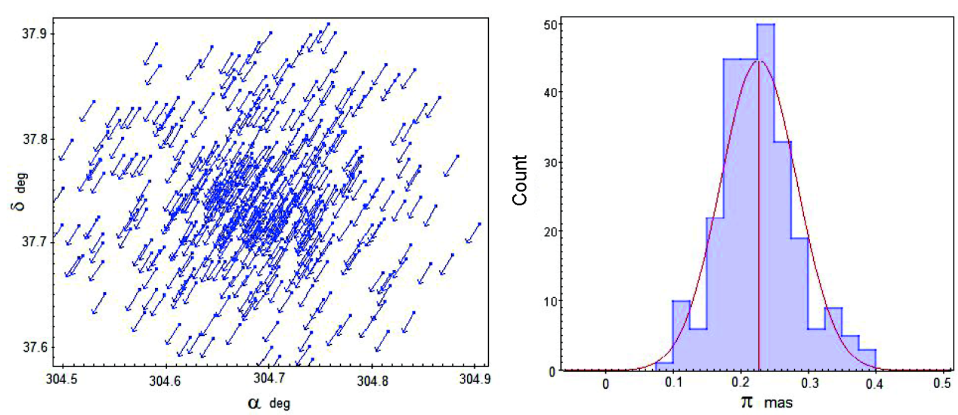

Fig. 4 The left panel shows the magnified velocities of cluster member candidates, i.e. the co-moving stars within the cluster area. They are located in the range of parallax of 0.1 mas $< \pi <$ 0.4 mas, which is presented in the right panel; the mean parallax = 0.23 $\pm$ 0.06 mas.

where $f_{\rm bg}$, f_0 and $r_{\rm c}$ are background, central densities of the stars in the cluster and the core radius of the cluster respectively. The angular limited radius is found to be $6.6'$ ($\sim$8.8 pc), while the core radius $r_{\rm c} = 1.8'$ ($\sim$2.4 pc). The concentration parameter of Peterson & King (1975) $C = \log(R_{\rm lim}/R_{\rm c}) \approx 0.6$.

4 COLOR-MAGNITUDE DIAGRAMS

CMDs of the cluster Dolidze 41 have been constructed using the *Gaia* DR2 bandpass $G \sim (BP - RP)$ as shown in the left panel of Figure 6, while the middle and right panels display the CMDs of the 2MASS bandpasses $J \sim (J - H)$ and $K \sim (J - K)$ respectively. Isochrones derived from *Gaia* data were obtained from CMD 3.0 with different ages and metallicities at *http://stev.oapd.inaf.it/cgi-bin/cmd_3.0*. All diagrams were fitted to the solar theoretical isochrones of Marigo et al. (2017). The 2MASS dataset has the benefits of being homogenized over the whole sky and covering near infrared wavelengths J (1.25 µm), H (1.65 µm) and $K_{\rm s}$ (2.16 µm), wherever young clusters can be observed in their nebulous environments. Isochrone fitting was started using some guesses of ages and metallicity ranges for the cluster. However, we used the photometric systems with solar metallicity, because most open cluster studies are based on isochrone fitting of solar metallicity Z = 0.0152 (Caffau et al. 2009, 2011) for simplicity and comparison (Yen et al. 2018). Best fitting isochrones were then used to estimate the parameters of Dolidze 41.

In Figure 6, the blue dots refer to co-moving stars in the cluster's area, located within the range of parallax for the cluster (0.1 mas $< \pi <$ 0.4 mas) and proper motion errors $\leq 10\%$, while the red dots indicate the stars with higher proper motion errors. The cyan dots represent the fore/background field stars in the cluster region. The age of the cluster is found to be 200 $\pm$ 10 Myr. The intrinsic distance modulus $(m - M)_{\rm o}$ = 13.3 $\pm$ 0.1 mag, which corresponds to a distance of 4625 $\pm$ 210 pc. The JHK photometric color excess $E(J - H)$ and $E(J - K)$ are found to be 0.35 and 0.55 mag respectively, which implies an optical reddening of $E(B - V) = 0.54$ mag. Correspondingly, the linear diameter, the distance from Galactic center R_g, the distance from the Galactic plane $Z_\odot$ and the distances $X_\odot$ and $Y_\odot$ from the Sun on the Galactic plane are found to be 17.7 pc, 8.5 kpc, 80 pc, 1140 pc and 4480 pc respectively; for more details about the calculations, see Tadross (2011).

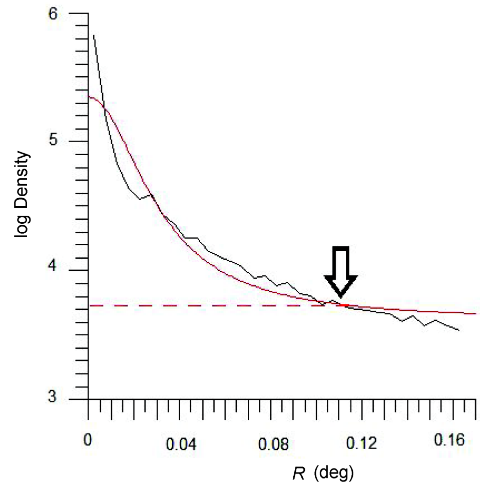

Fig. 5 The radial density profile of Dolidze 41. The model curve of King (1966) has been applied. The angular limited radius $R_{\rm lim}$ = 0.11° (6.6′, i.e. $\sim$8.8 pc). The core radius $r_{\rm c}$ = 0.03° (1.8′, i.e. $\sim$2.4 pc).

5 LUMINOSITY AND MASS FUNCTIONS, AND DYNAMICAL STATUS

An open cluster is composed of hundreds of stars having identical ages and compositions but different masses. The luminosity function and mass function (LF and MF respectively) depend principally on determination of the membership of the cluster. Here, member candidates are the co-moving stars located within the cluster's area, at intervals within the range of parallax, with proper motion errors $\leq 10\%$. Consequently, 480 stars in the cluster region are counted inside the limit diameter of 17.7 pc.

The stars have been counted in terms of the absolute magnitude $M_{\rm G}$ after applying the distance modulus derived above. The magnitude bin intervals are taken to be $\Delta M_{\rm G} = 0.50$ mag. The magnitude bin intervals incorporate a reasonable number of stars in every bin for the most effective potential statistics of LF and MF. To convert the star absolute magnitude to luminosity and mass, we use the theoretical tables of evolutionary tracks from Marigo et al. (2017) for the same cluster age. From the LF of Dolidze 41, we can infer that more massive stars are more centrally concentrated whereas the peak value lies at the fainter magnitude bin of $G \approx 18.0$ mag, i.e. $M_G \approx 4.7$ mag. The LF has been created as shown in Figure 7 (the gray histogram). In this context, the entire luminosity of the cluster is found to be ~ -4.3 mag. The LF and MF are correlated to each other according to the well-known mass-luminosity relation. Therefore, the MF distribution has been derived as shown in Figure 7 (the blue dots), whereas the red line refers to the initial mass

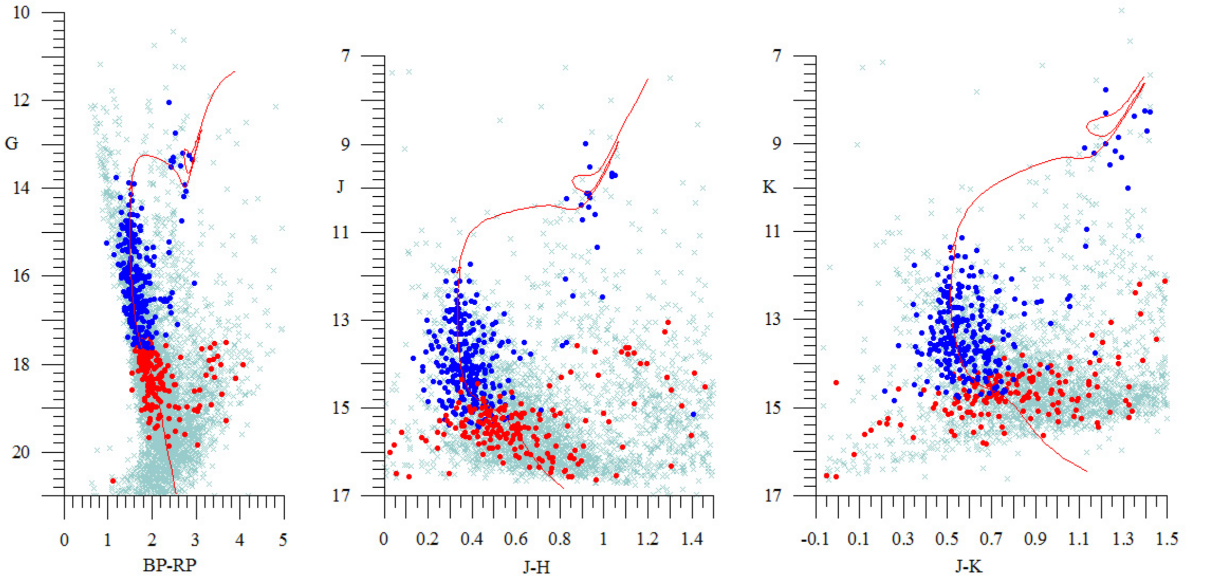

Fig. 6 CMDs of the cluster Dolidze 41: The *blue dots* refer to co-moving stars in the cluster's area, located within the range of parallax for the cluster, with proper motion errors less than 10%. The *red dots* indicate stars with higher proper motion errors. The *cyan dots* represent fore/background field stars around the cluster region. The left panel shows the CMD of *Gaia* DR2 bandpass $G \sim (BP - RP)$, while the middle and right panels display the CMDs of 2MASS bandpass $J \sim (J - H)$ and $K \sim (J - K)$ respectively. All diagrams are fitted to the theoretical solar isochrones of Marigo et al. (2017). The intrinsic distance modulus is found to be 13.3 $\pm$ 0.1 mag, and the color excess values $E(J - H)$ and $E(J - K)$ are 0.35 and 0.55 mag respectively. The age of the cluster is found to be 200 $\pm$ 10 Myr.

function (IMF) slope, which can be obtained from the subsequent equation

$$\frac{dN}{dM} \propto M^{-\alpha} \ , \tag{2}$$

where $\frac{dN}{dM}$ is the number of stars in the mass interval $[M : (M + dM)]$ and α is the slope of the relation $(\Gamma = -2.3 \pm 0.24)$ according to Salpeter (1955). We calculated the overall mass of the cluster by integrating the masses of the members (Sharma et al. 2006), which is found to be $640\, M_\odot$.

Knowing the overall mass of the cluster and applying the equation from Jeffries et al. (2001), the tidal radius can be derived as

$$R_{\rm t} = 1.46(M_{\rm c})^{1/3} \ , \tag{3}$$

where $R_{\rm t}$ and $M_{\rm c}$ are the tidal radius and the overall mass of the cluster respectively. $R_{\rm t}$ is calculated to be 12.6 pc.

Following Spitzer & Hart (1971), the dynamical relaxation time $T_{\rm R}$ is obtained from the relation

$$T_{\rm R} = \frac{8.9 \times 10^5 \sqrt{N} \times R_{\rm h}^{1.5}}{\sqrt{m} \times \log(0.4N)} \ , \tag{4}$$

where N is the number of cluster members, $R_{\rm h}$ is the radius containing half of the cluster mass in parsecs and m is the average mass of the cluster in solar units, assuming that $R_{\rm h}$ equals half of the cluster radius. Then, the

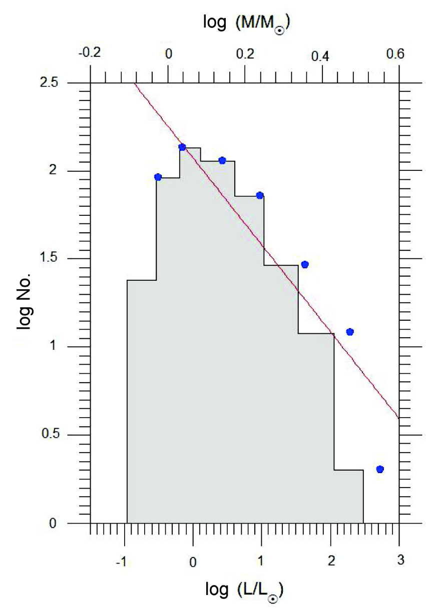

Fig. 7 The LF and MF of Dolidze 41. The *gray* histogram represents the luminosity distribution of the cluster, where the total luminosity is found to be -4.3 mag. The *blue points* refer to the mass distribution of the cluster and the *red line* shows the linear fitting, where the IMF slope is found to be –2.3 $\pm$ 0.24.

Table 1 Comparisons between the Previous and Present Results

Parameter	TN (2010)	Present work
pm $\alpha \cos \delta$	–	-2.95 ± 0.14 mas yr^{-1}
pm δ	–	-4.68 ± 0.14 mas yr^{-1}
Parallax	–	0.23 ± 0.06 mas
Age	400 Myr	200 Myr
Metal abundance	0.019	0.0152
$E(B-V)$	0.53 mag	0.54 mag
R_{v}	3.25	3.1
Intrinsic modulus	12.20 mag	13.30 ± 0.10 mag
Distance	1763 pc	4625 ± 210 pc
Limited radius	5.0′	6.6′ (8.8 pc)
Core radius	–	1.8′ (2.4 pc)
Tidal radius	–	12.6 pc
Membership	–	480 stars
R_g	8.2 kpc	8.5 kpc
$X_\odot$	–435 pc	1140 pc
$Y_\odot$	1708 pc	4480 pc
$Z_\odot$	31 pc	80 pc
Total luminosity	–	–4.3 mag
IMF slope	–	$\Gamma = -2.3 \pm 0.24$
Total mass	–	$\approx 640\ M_\odot$ (minimum)
Relaxation time	–	< 40 Myr
c	–	≈ 0.6
τ	–	≈ 6.0

relaxation time is found to be less than 40 Myr. The dynamical evolution parameter $\tau = \mathrm{Age}/T_{\mathrm{R}} \approx 6.0$, which means that the cluster Dolidze 41 is indeed dynamically relaxed.

6 CONCLUSIONS

The open cluster Dolidze 41 is a poorly studied object, and the only photometric study found in the literature was carried out by TN (2010) using the 2MASS database. According to our analysis for refining the fundamental parameters of Dolidze 41 in the *Gaia* era, we present a real astro-photometric study here, which is somewhat different from the previous one by TN (2010). The present and previous results are summarized and compared in Table 1.

Acknowledgements This work has made use of data from the European Space Agency (ESA) mission *Gaia* processed by the *Gaia* Data Processing and Analysis Consortium (DPAC), (*https://www.cosmos.esa.int/web/gaia/dpac/consortium*). Funding for the DPAC has been provided by national institutions, in particular the institutions participating in the *Gaia* Multilateral Agreement. In addition, the present study makes use of data products from the Two Micron All Sky Survey, which is a joint project of the University of Massachusetts and the Infrared Processing and Analysis Center/California Institute of Technology, funded by the National Aeronautics and Space Administration and the National Science Foundation. Virtual observatory tools like TOPCAT and ALADIN have been used in the analysis.

References

Bonnarel, F., Fernique, P., Bienaymé, O., et al. 2000, A&AS, 143, 33
Bragaglia, A. 2018, in IAU Symposium, 330, IAU Symposium, ed. A. Recio-Blanco, P. de Laverny, A. G. A. Brown, & T. Prusti, 119
Caffau, E., Maiorca, E., Bonifacio, P., et al. 2009, A&A, 498, 877
Caffau, E., Ludwig, H.-G., Steffen, M., Freytag, B., & Bonifacio, P. 2011, Sol. Phys., 268, 255
Dias, W. S., Monteiro, H., Caetano, T. C., et al. 2014, A&A, 564, A79
Gaia Collaboration, Brown, A. G. A., Vallenari, A., et al. 2018, arXiv:1804.09365
Jeffries, R. D., Thurston, M. R., & Hambly, N. C. 2001, A&A, 375, 863
Kazlauskas, A., Sperauskas, J., & Boyle, R. P. 2013, New Astron., 19, 34
Kharchenko, N. V., Piskunov, A. E., Schilbach, E., Röser, S., & Scholz, R.-D. 2013, A&A, 558, A53
King, I. R. 1966, AJ, 71, 64
Marigo, P., Girardi, L., Bressan, A., et al. 2017, ApJ, 835, 77
Peterson, C. J., & King, I. R. 1975, AJ, 80, 427
Salpeter, E. E. 1955, ApJ, 121, 161
Sharma, S., Pandey, A. K., Ogura, K., et al. 2006, AJ, 132, 1669
Skrutskie, M. F., Cutri, R. M., Stiening, R., et al. 2006, AJ, 131, 1163
Spitzer, Jr., L., & Hart, M. H. 1971, ApJ, 164, 399
Tadross, A. L. 2008a, MNRAS, 389, 285
Tadross, A. L. 2008b, New Astron., 13, 370
Tadross, A. L. 2009a, New Astron., 14, 200
Tadross, A. L. 2009b, Ap&SS, 323, 383
Tadross, A. L., & Nasser, M. A. 2010, arXiv:1011.2934
Tadross, A. L. 2011, Journal of Korean Astronomical Society, 44, 1
Taylor, M. B. 2005, in Astronomical Society of the Pacific Conference Series, 347, Astronomical Data Analysis Software and Systems XIV, eds. P. Shopbell, M. Britton, & R. Ebert, 29
Yen, S. X., Reffert, S., Röser, S., et al. 2018, in IAU Symposium, 330, eds. A. Recio-Blanco, P. de Laverny, A. G. A. Brown, & T. Prusti, 281